BIOCELL
2023 47(5): 1107-1115

Tech Science Press

Tanshinone IIA protects intestinal epithelial cells from ferroptosis through the upregulation of *GPX4* and *SLC7A11*

Han WANG[1,2,#]; Yang SUN[1,2,#]; Xiaoxu ZHANG[2,3]; Xiaoying WANG[4]; Yujun XIA[1,*]; Lisheng WANG[1,2,*]

[1] School of Basic Medicine, Qingdao University, Qingdao, 266071, China
[2] Laboratory of Molecular Diagnosis and Regenerative Medicine, The Affiliated Hospital of Qingdao University, Qingdao, 266000, China
[3] Department of Hematology, The Affiliated Hospital of Qingdao University, Qingdao, 266000, China
[4] Beijing Institute of Radiation Medicine, Beijing, 100850, China

Key words: Tanshinone IIA, *GPX4*, Ferroptosis, Intestinal epithelial cells, IBD

Abstract: Background: Inflammatory bowel disease (IBD) is a chronic inflammatory disease of the gastrointestinal tract. The destruction of the intestinal epithelial barrier is one of the major pathological processes in IBD pathology. Growing evidence indicated that epithelial cell ferroptosis is linked to IBD and is considered a target process. **Methods:** RAS-selective lethal 3 (RSL3) was used to induce ferroptosis in intestinal epithelial cell line No. 6 (IEC-6) cells, and cell ferroptosis and the effects of tanshinone IIA (Tan IIA) were determined by cell counting kit-8 (CCK-8), reactive oxygen species (ROS) staining, Giemsa staining and transmission electron microscope (TEM). The cell viability of natural product library compounds was determined by CCK-8. The expression of ferroptosis-related genes were detected by real-time quantitative polymerase chain reaction (RT-qPCR) and western blot. **Results:** Treatment of IEC-6 cells results in the accumulation of ROS and typical morphological characteristics of ferroptosis. RSL3 treatment caused rapid cellular cytotoxicity which could be reversed by ferrostatin-1 (Fer-1) in IEC-6 cells. Natural product library screening revealed that Tan IIA is a potent inhibitor of IEC-6 cell ferroptosis. Tan IIA could significantly protect the RSL3-induced ferroptosis of IEC-6 cells. Furthermore, the ferroptosis suppressors, glutathione peroxidase 4 (*GPX4*), solute carrier family 7 member 11 (*SLC7A11*), and miR-17-92 were found to be early response genes in RSL3-treated cells. Treatment of IEC-6 cells with Tan IIA resulted in upregulation of *GPX4*, *SLC7A11*, and miR-17-92. **Conclusion:** Our study demonstrated that Tan IIA protects IEC-6 cells from ferroptosis through the upregulation of *GPX4*, *SLC7A11*, and miR-17-92. The findings might provide a theoretical grounding for the future application of Tan IIA to treat or prevent IBD.

Introduction

Inflammatory bowel disease (IBD) is a chronic inflammatory disease with an unknown etiology (Ko and Auyeung, 2014). In the western world, the annual incidence of IBD is estimated to be 10–30 cases per 100,000 persons and these cases are usually accompanied by overweight and obesity (Singh *et al.*, 2017). IBD is caused by excessive inflammatory reactions, mucosa damage, and tissue disruption of the gut wall (Guan, 2019). The suppression of the immune responses may enhance healing and restore the physiological functions of the gut (Ihara *et al.*, 2017). Until now, there are no effective measures available to prevent and treat IBD. An extensive understanding of the pathological and physiological of cell death in the intestinal epithelium is critical to developing novel approaches for IBD treatment. Thus, novel cell death models of intestinal epithelial cells to screen effective medicine for IBD prevention and treatment are extremely important.

The occurrence and development of IBD are associated with the dysregulated immune response and damaged epithelial cell barrier (Gao *et al.*, 2018; Parikh *et al.*, 2019). Accumulating evidence have confirmed that epithelial cell death and its regulatory mechanisms are involved in both homeostasis and repair of the intestine. Epithelial cell death and its protection have been successfully applied to screen drugs for IBD prevention or therapy (Barbara *et al.*, 2021; Blander, 2016). Ferroptosis is a newly discovered cell

*Address correspondence to: Yujun Xia, xiayujun62@163.com; Lisheng Wang, lishengwang@qdu.edu.cn
#These authors contributed equally to this work
Received: 15 October 2022; Accepted: 16 January 2023

Doi: 10.32604/biocell.2023.027131

death that is iron-dependent and differs from traditional regulated cell death like apoptosis, pyroptosis, and necrosis (Dixon *et al.*, 2012; Stockwell *et al.*, 2017; Yang and Stockwell, 2016). Recently it is demonstrated that regulated cell death such as ferroptosis and pyroptosis are linked to the damage of epithelial barriers and are involved in IBD pathogenesis (Cai *et al.*, 2021; Gao *et al.*, 2021; Rana *et al.*, 2022; Xu *et al.*, 2021). Inhibiting ferroptosis may become a novel approach for IBD therapeutics (Huang *et al.*, 2022). However, the detailed molecular mechanisms of intestinal epithelial cell ferroptosis have not been extensively explored.

Intestinal epithelial cell ferroptosis is an ideal model for screening inhibitors to develop effective drugs for IBD therapy (Subramanian *et al.*, 2020). When screening a natural product library for epithelial cells ferroptosis inhibitors, we found the tanshinone IIA (Tan IIA), an effective inhibitor of RAS-selective lethal 3 (RSL3)-induced ferroptosis in epithelial cells. Tanshinone is an important natural compound isolated from Salvia miltiorrhiza Bunge with various biological functions (Estolano-Cobián *et al.*, 2021). Tan IIA, one of the major lipophilic components, is the most abundant lipophilic compound in Danshen. Previous reports suggested that Tan IIA is a potential agent for IBD treatment and prevention (Zhang *et al.*, 2015; Zhu *et al.*, 2022). Tan IIA interferes with IBD pathogenesis by inhibiting epithelial cell death including apoptosis (Guan *et al.*, 2021). Tan IIA protects human endothelial cells in the coronary artery from lipid peroxidation-induced ferroptosis by activating the *NRF2* pathway (He *et al.*, 2021). However, the anti-ferroptosis role of Tan IIA in intestinal epithelial cells and its mechanisms have not been explored. In this study, we established an epithelial cell ferroptosis model by using RSL3-treated intestinal epithelial cell line No. 6 (IEC-6) cells and screened Tan IIA as the anti-ferroptosis inhibitor. Further, its biological effects on ferroptosis and extensive mechanisms were explored.

Materials and Methods

Cell culture

The rat intestinal epithelial cell line No. 6 (IEC-6) was provided by iCell Bioscience Inc (Shanghai, China). The cells were cultured in Dulbecco's Modified Eagle Medium (Procell, Wuhan, China) supplemented with 10% fetal bovine serum (Procell) and 0.1 U/mL insulin (MedChemExpress, New Jersey, USA) in a humidified atmosphere at 37°C with 5% CO_2.

Cell viability assay

Cell viability was measured using cell counting kit-8 (CCK-8) solution (Bimake, Houston, Texas, USA) following instructions of the manufacturer. IEC-6 cells were seeded (1×10^4 cells) into 96-well plates containing 100 μL complete medium per well, treated with RSL3 (MedChemExpress). Ferrostatin-1 (Fer-1) (MedChemExpress) was used as the positive control. Then, to each well, 10 μL CCK-8 solution was added and incubated at 37°C for 2 h in a dark place. The absorbance level was measured at 450 nm using a microplate reader (Molecular Devices, USA). The cell viability was calculated based on the control group.

Compound library screening

The compound library, which included 66 natural small molecule compounds were purchased from APExBIO Technology (Houston, Texas, USA). The IEC-6 cells (1×10^4 cells) were seeded into 96-well plates in 100 μL complete medium per well, which were treated with 0.5 μM RSL3 and 2.5 μM natural small molecule compounds for 48 h. Fer-1 was used as the positive control. The cell viability was measured by the CCK-8 assay.

Real-time quantitative polymerase chain reaction (qRT-PCR)

Total RNA was extracted from IEC-6 cells using TRIzol reagent (Invitrogen, Carlsbad, CA, USA). The RNA concentration was detected by measuring the absorbance at 260 and 280 nm using a microplate reader (Molecular Devices, San Jose, USA). cDNA was synthesized using TransScript® One-step cDNA synthesis kit (Transgen, Beijing, China) from 1 μg total RNA for detection of genes coding for GSH-dependent peroxidase 4 (*GPX4*) and solute carrier family 7 member 11 (*SLC7A11*), and qRT-PCR reactions were amplificated by SYBR Green qPCR SuperMix kit (Transgen). The qRT-PCR analysis for expression of the miR-17-92 cluster, including miR-17, miR-18a, miR-19a, miR-19b, miR-20a, and miR-92a was conducted with the miRNA 1st strand cDNA synthesis kit (Accurate Biotechnology, Beijing, China) and amplified by SYBR Green Pro Taq HS qPCR Kit II (Accurate Biotechnology). A total of 40 cycles were set for the qPCR reaction, including 95°C, 30 s for denaturation, 95°C, 5 s for annealing, and 60°C, 30 s for the extension. Cycle threshold (Ct) values of genes were determined by Applied Biosystems QuantStudio 5 (Thermo Fisher, Waltham, USA). β-actin was used as the internal reference of *GPX4* and *SLC7A11*. U6 was used as the internal reference of the miR-17-92 cluster. The relative level of mRNA and miRNA expressions were calculated using the $2^{-\Delta\Delta CT}$ method. Primers of the miR-17-92 cluster, U6, *GPX4*, *SLC7A11*, and *β-actin* were designed and synthesized by Sangon Biotech (Beijing, China) and their sequences are mentioned in Table 1.

TABLE 1

Specific primers in used for real-time-quantitative polymerase chain reaction

Gene	Direction sequence (5′-3′)
Has-miR-92a-3p	TATTGCACTTGTCCCGGCCT
Has-miR-20a-5p	CGCGTAAAGTGCTTATAGTGCAGGTAG
Has-miR-17-3p	CACTGCAGTGAAGGCACTTGTAG
Has-miR-17-5p	GCAAAGTGCTTACAGTGCAGGTAG
Has-miR-18a-3p	ACTGCCCTAAGTGCTCCTTCTG
Has-miR-19b-3p	TCGTGTGCAAATCCATGCAAAACTGA
U6	Forward: GCTTCGGCAGCACATATACTAAAAT Reverse: CGCTTCACGAATTTGCGTGTCAT
GPX4	Forward: ATAAGAACGGCTGCGTGGTGAAG

(Continued)

Table 1 (continued)

Gene	Direction sequence (5′-3′)
	Reverse: TAGAGATAGCACGGCAGGTCCTTC
SLC7A11	Forward: CCATCATCATCGGCACCGTCATC
	Reverse: TACTCCACAGGCAGACCAGAACAC
β-actin	Forward: CCGGGACCTGACAGACTA
	Reverse: GTTTCATGGATGCCACAGGAT

Measurement of reactive oxygen species (ROS) production

IEC-6 cells were harvested and counted, then every well of 6-well plates was seeded with 5×10^5 cells and cultured for 6 h with or in the absence of RSL3, and the concentration of Tan IIA was set at 5 and 2.5 μM. Cells were digested with trypsin, collected by centrifuge, labeled with 2′,7′-Dichlorofluorescein diacetate (DCFH-DA) probe (Elabscience, Wuhan, China), at 10 μM concentration, and incubated at 37°C in dark for 30 min. Finally, cells were labeled with 7-aminoactinomycin D (7-AAD) viability staining solution (BioLegend, San Diego, CA, USA). Dead cells were excluded from the collected cells by the APC channel and the ROS level was detected by the FITC channel using CytoFLEX (Beckman Coulter, CA, USA).

Giemsa staining assay

After IEC-6 cells were treated with RSL3, Fer-1, and Tan IIA, cells were fixed with methanol for 2 min. Then, the cells were washed twice with phosphate-buffered saline (PBS) and stained at room temperature for 20 min by Giemsa solution (Solarbio, Beijing, China). Finally, the Giemsa solution was discarded and the cells were washed with PBS. The cell morphology was observed and photographed by an optical microscope (Leica, Germany).

Transmission electron microscopy (TEM)

IEC-6 cells were cultured with RSL3 and Tan IIA for 24 h, then cells were fixed with TEM fixative solution (Servicebio, Wuhan, China). The TEM preparation and cell morphology observation were conducted by Servicebio Technology.

Western blotting

IEC-6 cells were cultured with RSL3 and Tan IIA and lysed with RIPA (Meilunbio, Dalian, China) containing 1%

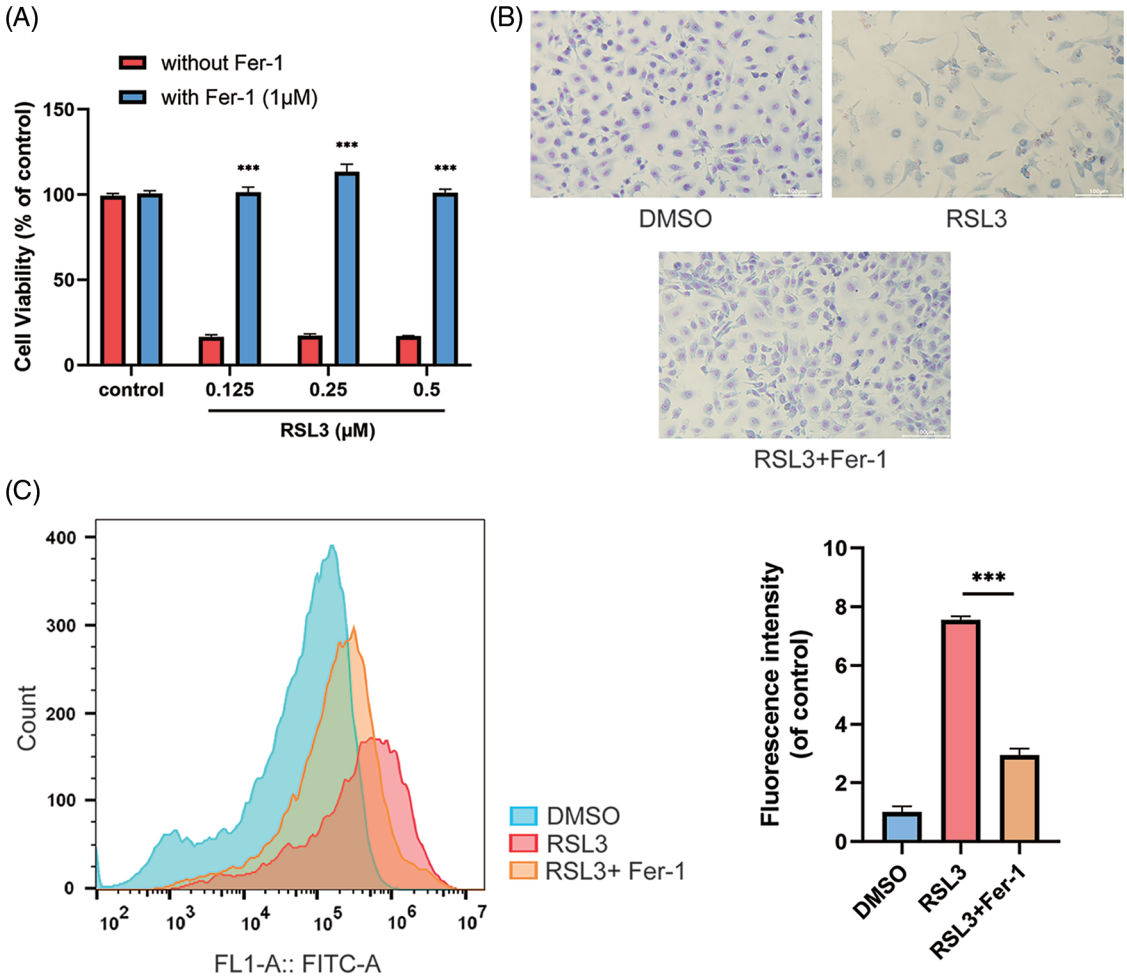

FIGURE 1. RAS-selective lethal 3 (RSL3) induced ferroptosis of IEC-6 cells. (A) Effect of Fer-1 (1 μM) on the lethality of IEC-6 cells treated with RSL3 at different concentrations (0.125, 0.25, 0.5 μM) or (DMSO; control) for 24 h by CCK-8 assay, ***$p < 0.001$ *vs.* control group. (B) Morphology of IEC-6 cells treated with RSL3 (0.5 μM) or DMSO (control) in the presence or absence of Fer-1 (1 μM); magnification: 20×, scale bars: 200 μm. (C) Effect of Fer-1 (1 μM) on RSL3 (0.5 μM)-induced ROS production in IEC-6 cells after 6 h treatment, ***$p < 0.001$ *vs.* RSL3 group. IEC-6, intestinal epithelial cell line No. 6; DMSO, dimethylsulfoxide; CCK-8, cell counting kit 8; Fer-1, ferrostatin-1; ROS, reactive oxygen species.

phenylmethanesulfonyl fluoride (Meilunbio) on ice. Protein concentration was measured by BCA Protein Assay Kit (Solarbio). A total of 20 μg protein was separated by 12% sodium dodecyl sulfate-polyacrylamide gel electrophoresis (Yeasen, Shanghai, China) and transferred to a polyvinylidene fluoride membrane (Millipore, Germany). Then membranes were blocked with 5% defatted milk for 1 h and labeled with primary antibodies (β-actin, ABclonal, Wuhan, China; SLC7A11, ABclonal; GPX4, Cell Signaling, Danvers, Massachusetts, USA) overnight at 4°C. Subsequently, membranes were incubated with goat anti-rabbit IgG H&L (horseradish peroxidase) secondary antibody (ZSGB-Bio, Beijing, China) and visualized by adding enhanced chemiluminescence solution (Yeasen). The protein bands were analyzed by the ProteinSimple instrument (Bio-Techne, Minnesota, USA).

Statistical analysis

Data were analyzed with GraphPad Prism version 9.0 software (La Jolla, CA, USA). All results were expressed as mean ± SD. Differences between the two groups were analyzed by paired *t*-test. p-value < 0.05 was considered as statistical significance.

Results

RAS-selective lethal 3 induces typical ferroptosis in IEC-6 cells

RSL3 ((1S,3R)-RSL3) is an inhibitor of *GPX4* (ferroptosis activator) and induces ferroptotic death in numerous cell types. To set up a ferroptosis model of intestinal epithelial cells, we treated IEC-6 cells with different concentrations of RSL3 and observed the RSL3-induced cell death. CCK-8 assay revealed that RSL3 treatment, even at low concentrations of 0.125 μM, significantly reduced cell viability of IEC-6 cells. Ferrostatin-1 (Fer-1), a specific ferroptosis inhibitor, could significantly rescue RSL3-induced cell death (Fig. 1A) and Giemsa staining of RSL3-treated cells revealed typical ferroptotic morphological changes, such as cell volume shrinkage, cell membrane disruption, the cell morphology (Fig. 1B). Ferroptosis is characterized by the production of plasma membrane phospholipid peroxide-induced by ROS in iron-mediated Fenton reactions. RSL3 treatment caused a rapid generation of ROS in IEC-6 cells, which could be reversed by Fer-1. Thus, RSL3-induced IEC-6 cell death is a typical ferroptosis model of epithelial cells (Fig. 1C).

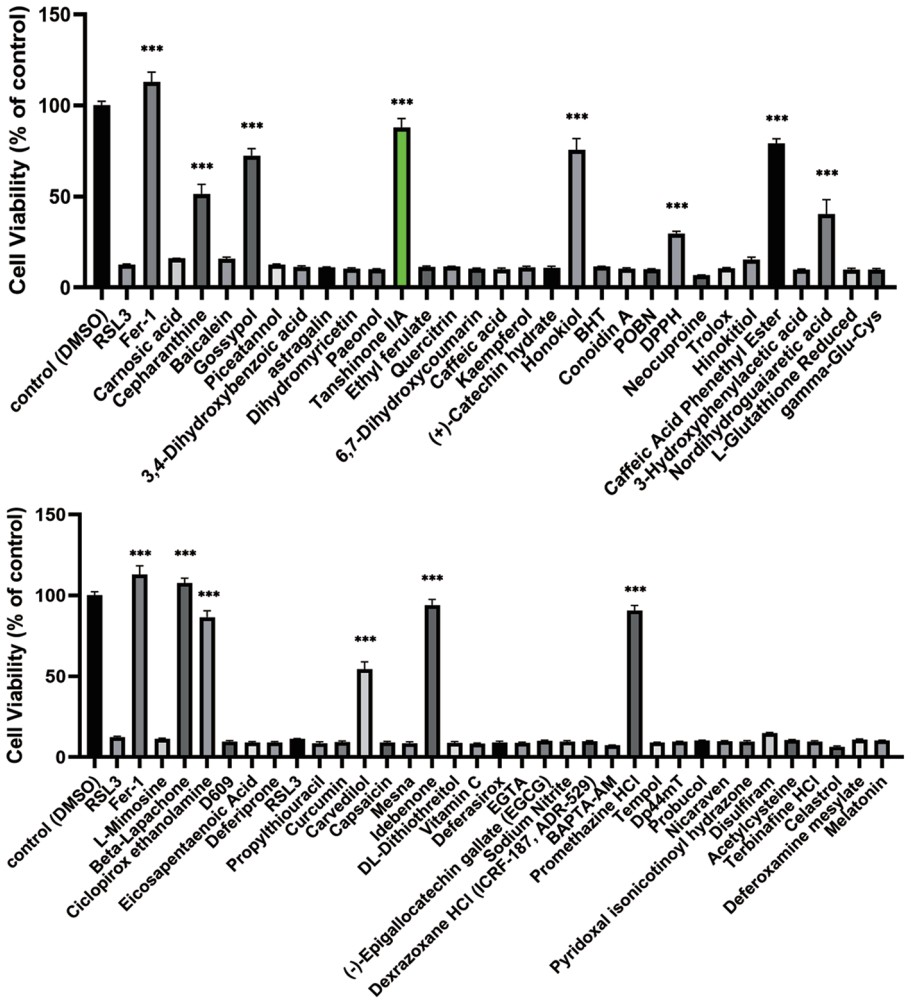

FIGURE 2. Identification of Tan IIA as an inhibitor of RAS-selective lethal 3 (RSL3)-induced ferroptosis in IEC-6 cells. IEC-6 cells were assayed for cell viability after being treated with 0.5 μM RSL3 and 2.5 μM natural product compounds for 48 h. The control group was treated with DMSO (control). The cell viability was determined by CCK8 assay. ***p < 0.001 *vs.* control group. IEC-6, intestinal epithelial cell line No. 6; DMSO, dimethylsulfoxide; CCK-8, cell counting kit 8.

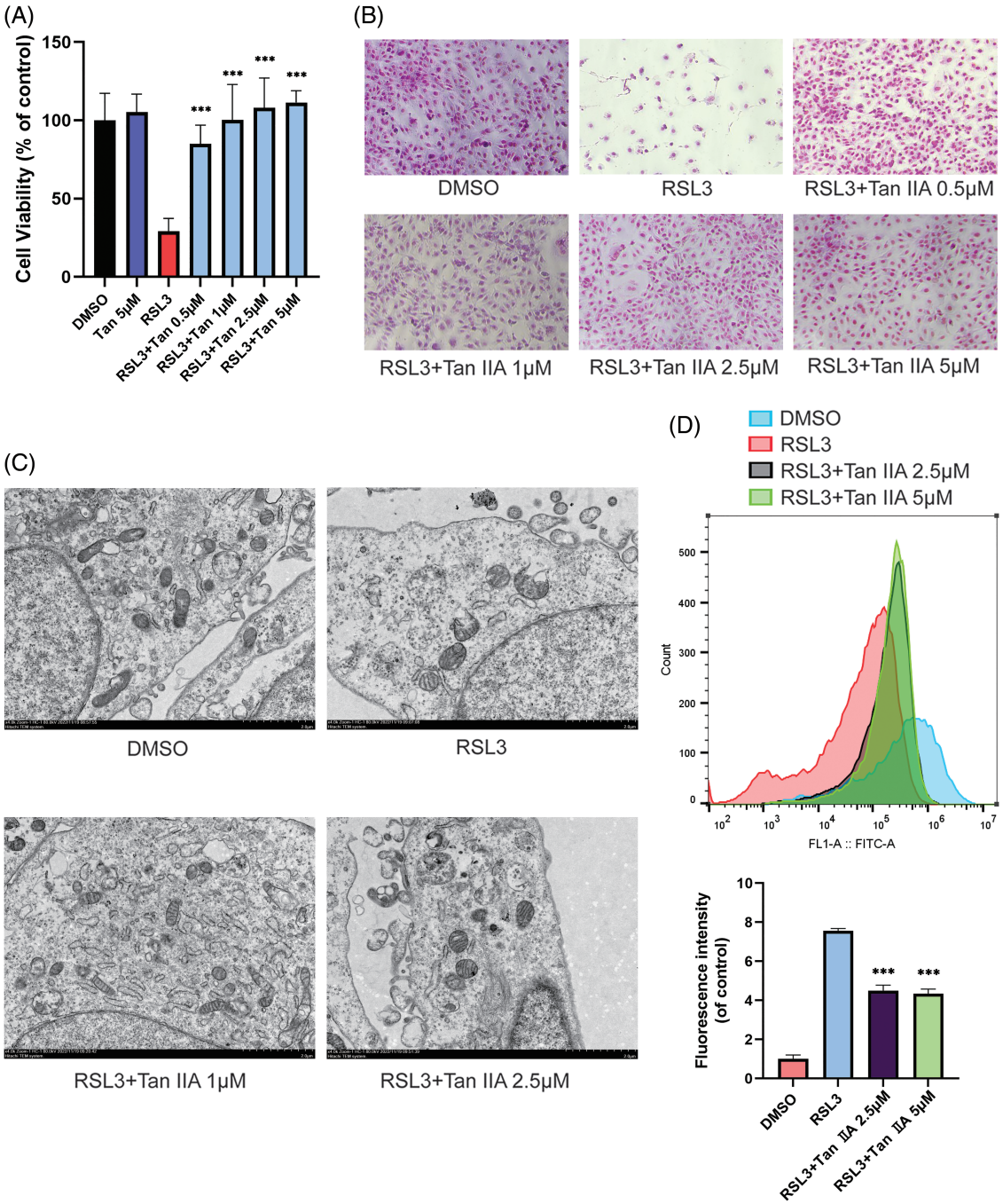

FIGURE 3. Tan IIA protected IEC-6 cells from RAS-selective lethal 3 (RSL3)-induced ferroptosis. (A) IEC-6 cells were treated with Tan IIA at indicated concentrations in the presence or absence of RSL3, and the cell viability was determined by CCK8 assay. ***$p < 0.001$ *vs*. RSL3 group. (B) IEC-6 cells were treated with 0.5 μM RSL3 in the presence or absence of Tan IIA, these cells were stained with Giemsa and photographed; magnification: 20×, scale bars: 200 μm. (C) TEM observation of IEC-6 cells cultured with RSL3 with or in the absence of Tan IIA (scale bars: 2.0 μm). (D) Effect of Tan IIA (5 μM and 2.5 μM) on RSL3 (0.5 μM)-induced ROS production in IEC-6 cells after 6 h of treatment, ***$p < 0.001$ *vs*. RSL3 group. IEC-6, intestinal epithelial cell line No. 6; CCK-8, cell counting kit 8; ROS, reactive oxygen species; TEM, transmission electron microscope.

Identification of Tan IIA as an inhibitor of RAS-selective lethal 3-induced epithelial cell ferroptosis

To identify the inhibitors of RSL3-induced ferroptosis, we screened a small natural product library from APExBIO with 66 compounds in IEC-6 cells. Cell viability was measured using CCK-8 in IEC-6 cells following treatment with 2.5 μM natural product compounds for 48 h. Twelve compounds were screened to protect the IEC-6 cells from RSL3-induced cell ferroptosis (Fig. 2). Among these, Tan IIA was shown to significantly reverse RSL3-induced ferroptosis.

Tan IIA suppresses RAS-selective lethal 3-induced ferroptosis of IEC-6 cells

Then we treated IEC-6 cells with different concentrations of Tan IIA in the presence of RSL3. CCK-8 assay and Giemsa

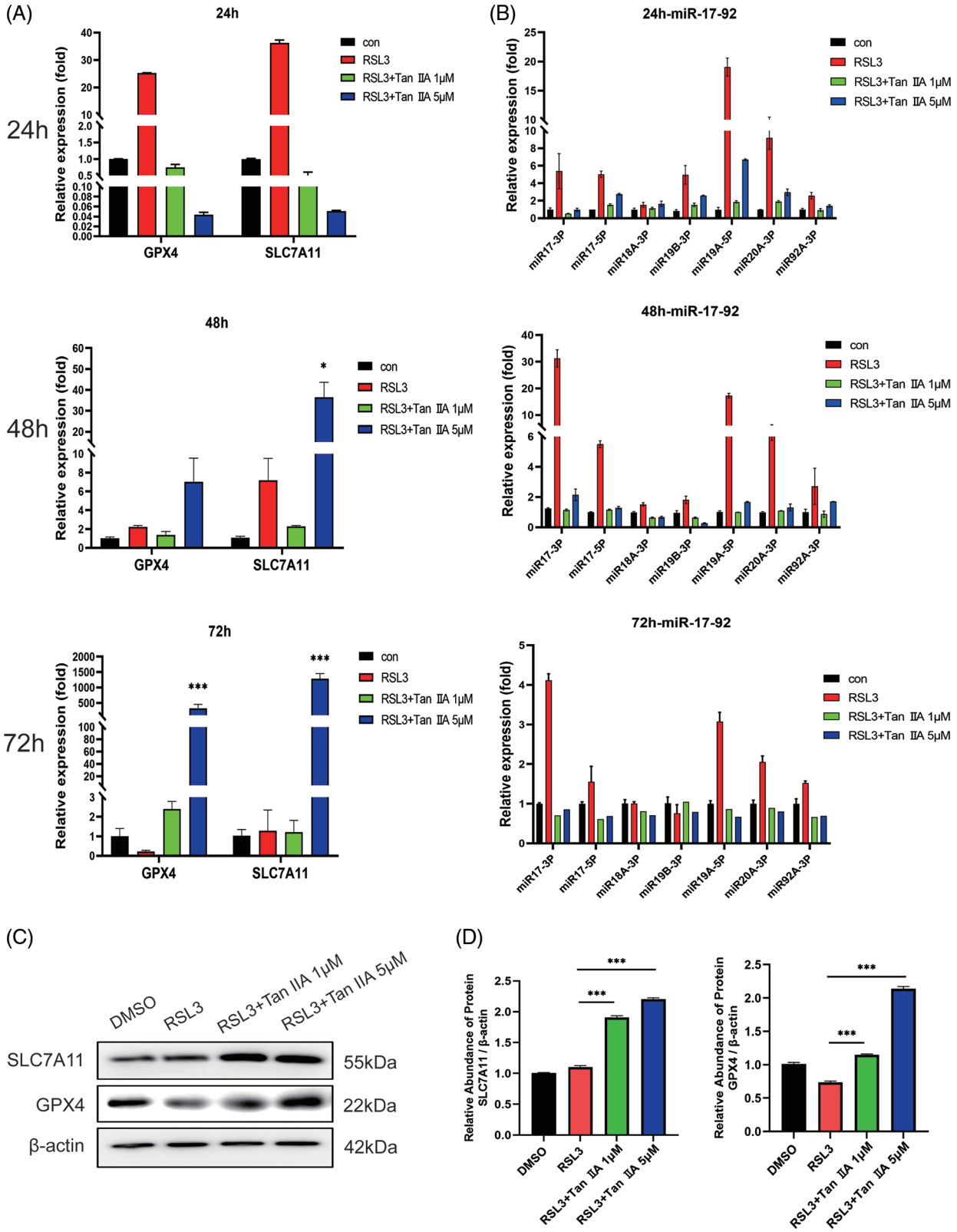

FIGURE 4. Tan IIA upregulated *GPX4*, *SLC7A11* and miR-17-92 expression in the RSL3-treated IEC-6 cells. (A, B) IEC-6 cells were treated with Tan IIA at a concentration of 1 and 5 μM in the presence of 0.25 μM RSL3 for 24, 48, and 72 h, and the expression of *GPX4*, *SLC7A11*, and miR-17-92 were determined by qRT-PCR, (C) Protein levels of *GPX4* and *SLC7A11* were detected by western blotting (24 h). (D) The relative abundance of proteins by gray values. β-actin was used as the internal control. $^{*}p < 0.05$, $^{***}p < 0.001$ *vs*. RSL3 group. IEC-6, intestinal epithelial cell line No. 6; *GPX4*, glutathione peroxidase 4, RSL-3, RAS-selective lethal 3; *SLC7A11*, solute carrier family 7 member 11; qRT-PCR, quantitative real-time polymerase chain reaction.

staining revealed that Tan IIA could rescue RSL3-induced cell death at a concentration of 0.5 μM. Tan IIA could not stimulate the growth of IEC-6 cells even at a high concentration of 5 μM, whereas Tan IIA significantly protected IEC-6 cells from RSL3-induced ferroptosis even at a low concentration of 0.5 μM (Fig. 3A). Fig. 3B shows the morphological characteristics of RSL3-treated IEC-6 cells in the presence or absence of Tan IIA by Giemsa staining. Furthermore, examination of microstructures of cells by TEM (Fig. 3C) revealed that RSL3-induced cell mitochondrial shrinkage and membrane disruption, the inner cristae of mitochondria were reduced or absent. Thus, both Fer-1 and Tan IIA protected the IEC-6 cells from ferroptosis. Moreover, Tan IIA decreased the ROS level in RSL3-induced IEC-6 cells (Fig. 3D).

Tan IIA upregulates glutathione peroxidase 4, solute carrier family 7 member 11, and miR-17-92 expression

Ferroptosis suppressors such as *GPX4*, *SLC7A11*, and miR-17-92 have been proven to inhibit ferroptosis of endothelial cells (Bai *et al.*, 2020; Xiao *et al.*, 2019). The expression of these genes in RSL3-treated IEC-6 cells in the presence of Tan IIA was further investigated. *GPX4*, *SLC7A11* and miR-17-92 function as RSL3 response genes in IEC-6 cells. The expressions of *GPX4* and *SLC7A11* are shown in Fig. 4A, and miR-17-92 cluster expressions at 24, 48, and 72 h are shown in Fig. 4B. RSL3 treatment significantly induced the expression of these genes within 24 h. Treatment of IEC-6 cells with 5 μM Tan IIA significantly upregulated *GPX4* and *SLC7A11* until 48 and 72 h, and also partly upregulated miR-17-92 expression. Moreover, Tan IIA treatment upregulated the levels of *GPX4* and *SLC7A11* proteins (Figs. 4C and 4D). Therefore, *GPX4* and *SLC7A11* might mediate the suppression of epithelial cell ferroptosis induced by Tan IIA.

Discussion

Emerging evidence suggests that iron accumulations and ferroptosis play a key role in the pathological progression of a large number of diseases of the digestive system such as metabolic-associated fatty liver disease, drug-induced liver injury, alcoholic liver disease, and colitis (Maras *et al.*, 2018; Qi *et al.*, 2020). Ferroptosis, a recognized mechanism of programmed cell death that is biochemically characterized by the accumulation of lipid peroxides and ROS (Stockwell and Jiang, 2020), might cause the disorder of epithelial cell death and play a significant role in the pathological process of IBD. Thus targeting ferroptosis can potentially become a novel therapeutic approach in the treatment of IBD (Huang *et al.*, 2022). Ferroptosis occurs in the intestine of patients with IBD. Currently, the lack of ferroptosis cell models has limited the screening of effective inhibitors for IBD treatment. IEC-6 cells were harvested from adult rat intestinal crypt cells and considered as a model for studying the intestine epithelial barriers. Treatment of IEC-6 cells with RSL3 resulted in typical ferroptosis-induced morphological changes, including cell volume shrinkage, mitochondrial shrinkage, and cell membrane disruption. In addition, RSL3-treated IEC-6 cells also exhibited high ROS activity and cellular toxicity which could be reversed by the ferroptosis inhibitor, Fer-1. Thus RSL3-treated IEC-6 cells might be an ideal model for the screening and validation of IBD therapeutic drugs. By using the RSL3-induced the ferroptosis model of IEC cells, we found that Tan IIA protected IEC-6 cells against ferroptosis. As far as we know, this study is the first to use the ferroptosis model to identify inhibitors of intestinal cell ferroptosis, and we also found that Tan IIA might have the potential application in IBD therapy.

Tan IIA, a pharmacologically active compound isolated from the rootstock of the Chinese herb Salvia miltiorrhiza Bunge (Danshen), has been widely used against several cardiovascular diseases, such as cardiomyopathy, arrhythmia, and congenital heart defects (Guo *et al.*, 2020). Tan IIA alleviates endoplasmic reticulum stress-induced cardiomyocyte apoptosis (Feng *et al.*, 2016). Multiple signal transduction pathways such as toll-like receptor/nuclear factor-kappaB (NF-κB), mitogen-activated protein kinases/NF-κB, and AMP-activated protein kinases/mTOR-dependent autophagy pathways were found to be involved in Tan IIA-induced cellular responses (Zhang *et al.*, 2019). Tan IIA therapy decreased the production of inflammatory mediators and restored aberrant signaling pathways in IBD (Zhang *et al.*, 2015). The anti-ferroptosis role of Tan IIA in intestinal epithelial cells might reveal the extensive mechanisms of its action in the therapy of IBD.

GPX4 is a ferroptosis activator in multiple types of cells by acting on mitochondrial voltage-dependent anion channel, blocking *GPX4* and targeting System Xc^- cystine/glutamate antiporter (Seibt *et al.*, 2019). In the system Xc^- containing subunits *SLC7A11* and *SLC3A2*, *SLC7A11* plays a vital role in cystine uptake (Liu *et al.*, 2019). Inhibition of *GPX4* and *SLC7A11* leads to the accumulation of ROS and the breakdown of redox homeostasis (Feng *et al.*, 2022). Mayr *et al.* (2020) have confirmed that small intestinal epithelial cells exhibit impaired *GPX4* activity and signs of lipid peroxidation in IBD. The NF-κB inhibitor pyrrolidine dithiocarbamate exhibits an antioxidant and anti-inflammatory function through multiple signals, including *GPX4* upregulation in the colitis model (Yin *et al.*, 2015). MicroRNAs are involved in a number of biological processes and are associated with ferroptosis (Xie and Guo, 2021). Among them, the polycistronic miR-17-92 cluster functions as a ferroptosis suppressor in endothelial cells. *A20* is a TNF-α-induced molecule that functions as a negative regulator of cell growth (Priem *et al.*, 2020). MiR-17-92 was proven to protect endothelial cells from erastin-induced ferroptosis through the *A20-ACSL4* axis (Xiao *et al.*, 2019). This study provides evidence that these ferroptosis suppressors are induced by RSL3 as the response gene, and Tan IIA could significantly protect the IEC-6 ferroptosis through regulation of *GPX4*, *SLC7A11*, and miR-17-92 expression.

Taken together, we screened Tan IIA as a ferroptosis inhibitor of IEC-6 cells. Tan IIA protects intestinal epithelial cells from ferroptosis through the upregulation of multiple suppressors and might provide a theoretical basis for the future application of Tan IIA for the prevention and treatment of IBD.

Funding Statement: This work was supported by the National Key Research and Development Program (Grant Number: 2017YFA0105303) and the Natural Science Foundation of Shandong Province (Grant Number: ZR2020MH327).

Author Contributions: The authors confirm their contribution to the paper as follows: study conception and design: Li-Sheng Wang, Yu-Jun Xia, and Han Wang; experimentation: Han Wang, Yang Sun, Xiao-Ying Wang, and Xiao-Xu Zhang; analysis and interpretation of results: Yang Sun and Xiao-Xu Zhang; draft manuscript preparation: Li-Sheng Wang, Yu-Jun Xia, and Yang Sun. All authors have reviewed the results and approved the final version of the manuscript.

Availability of Data and Materials: The datasets generated during and/or analysed during the current study are available from the corresponding author on reasonable request.

Ethics Approval: Not applicable.

Conflicts of Interest: The authors declare that they have no conflicts of interest to report regarding the present study.

References

Bai T, Li M, Liu Y, Qiao Z, Wang Z (2020). Inhibition of ferroptosis alleviates atherosclerosis through attenuating lipid peroxidation and endothelial dysfunction in mouse aortic endothelial cell. *Free Radical Biology & Medicine* **160**: 92–102. https://doi.org/10.1016/j.freeradbiomed.2020.07.026

Barbara G, Barbaro MR, Fuschi D, Palombo M, Falangone F, Cremon C, Marasco G, Stanghellini V (2021). Inflammatory and microbiota-related regulation of the intestinal epithelial barrier. *Frontiers in Nutrition* **8**: 718356. https://doi.org/10.3389/fnut.2021.718356

Blander JM (2016). Death in the intestinal epithelium-basic biology and implications for inflammatory bowel disease. *The FEBS Journal* **283**: 2720–2730. https://doi.org/10.1111/febs.13771

Cai X, Zhang Z, Yuan J, Ocansey D, Tu Q, Zhang X, Qian H, Xu W, Qiu W, Mao F (2021). hucMSC-derived exosomes attenuate colitis by regulating macrophage pyroptosis via the miR-378a-5p/NLRP3 axis. *Stem Cell Research & Therapy* **12**: 416. https://doi.org/10.1186/s13287-021-02492-6

Dixon S, Lemberg K, Lamprecht M, Skouta R, Zaitsev E et al. (2012). Ferroptosis: An iron-dependent form of nonapoptotic cell death. *Cell* **149**: 1060–1072. https://doi.org/10.1016/j.cell.2012.03.042

Estolano-Cobián A, Alonso MM, Díaz-Rubio L, Ponce CN, Córdova-Guerrero I, Marrero JG (2021). Tanshinones and their derivatives: Heterocyclic ring-fused diterpenes of biological interest. *Mini Reviews in Medicinal Chemistry* **21**: 171–185. https://doi.org/10.2174/1389557520666200429103225

Feng J, Li S, Chen H (2016). Tanshinone IIA ameliorates apoptosis of cardiomyocytes induced by endoplasmic reticulum stress. *Experimental Biology and Medicine* **241**: 2042–2048. https://doi.org/10.1177/1535370216660634

Feng Z, Qin Y, Huo F, Jian Z, Li X, Geng J, Li Y, Wu J (2022). NMN recruits GSH to enhance GPX4-mediated ferroptosis defense in UV irradiation induced skin injury. *Biochimica et Biophysica Acta (BBA)—Molecular Basis of Disease* **1868**: 166287. https://doi.org/10.1016/j.bbadis.2021.166287

Gao X, Cao Q, Cheng Y, Zhao D, Wang Z et al. (2018). Chronic stress promotes colitis by disturbing the gut microbiota and triggering immune system response. *Proceedings of the National Academy of Sciences of the United States of America* **115**: E2960–E2969. https://doi.org/10.1073/pnas.1720696115

Gao W, Zhang T, Wu H (2021). Emerging pathological engagement of ferroptosis in gut diseases. *Oxidative Medicine and Cellular Longevity* **2021**: 4246255. https://doi.org/10.1155/2021/4246255

Guan Q (2019). A comprehensive review and update on the pathogenesis of inflammatory bowel disease. *Journal of Immunology Research* **2019**: 7247238. https://doi.org/10.1155/2019/7247238

Guan R, Yao H, Li Z, Qian J, Yuan L et al. (2021). Sodium tanshinone IIA sulfonate attenuates cigarette smoke extract-induced mitochondrial dysfunction, oxidative stress, and apoptosis in alveolar epithelial cells by enhancing SIRT1 pathway. *Toxicological Sciences* **183**: 352–362. https://doi.org/10.1093/toxsci/kfab087

Guo R, Li L, Su J, Li S, Duncan SE, Liu Z, Fan G (2020). Pharmacological activity and mechanism of tanshinone IIA in related diseases. *Drug Design, Development and Therapy* **14**: 4735–4748. https://doi.org/10.2147/dddt.S266911

He L, Liu Y, Wang K, Li C, Zhang W, Li Z, Huang X, Xiong Y (2021). Tanshinone IIA protects human coronary artery endothelial cells from ferroptosis by activating the NRF2 pathway. *Biochemical and Biophysical Research Communications* **575**: 1–7. https://doi.org/10.1016/j.bbrc.2021.08.067

Huang J, Zhang J, Ma J, Ma J, Liu J, Wang F, Tang X (2022). Inhibiting ferroptosis: A novel approach for ulcerative colitis therapeutics. *Oxidative Medicine and Cellular Longevity* **2022**: 9678625. https://doi.org/10.1155/2022/9678625

Ihara S, Hirata Y, Koike K (2017). TGF-β in inflammatory bowel disease: A key regulator of immune cells, epithelium, and the intestinal microbiota. *Journal of Gastroenterology* **52**: 777–787. https://doi.org/10.1007/s00535-017-1350-1

Ko JK, Auyeung KK (2014). Inflammatory bowel disease: Etiology, pathogenesis and current therapy. *Current Pharmaceutical Design* **20**: 1082–1096. https://doi.org/10.2174/13816128113199990416

Liu T, Jiang L, Tavana O, Gu W (2019). The deubiquitylase OTUB1 mediates ferroptosis via stabilization of SLC7A11. *Cancer Research* **79**: 1913–1924. https://doi.org/10.1158/0008-5472.CAN-18-3037

Maras J, Das S, Sharma S, Sukriti S, Kumar J et al. (2018). Iron-overload triggers ADAM-17 mediated inflammation in severe alcoholic hepatitis. *Scientific Reports* **8**: 10264. https://doi.org/10.1038/s41598-018-28483-x

Mayr L, Grabherr F, Schwärzler J, Reitmeier I, Sommer F et al. (2020). Dietary lipids fuel GPX4-restricted enteritis resembling Crohn's disease. *Nature Communications* **11**: 1775. https://doi.org/10.1038/s41467-020-15646-6

Parikh K, Antanaviciute A, Fawkner-Corbett D, Jagielowicz M, Aulicino A et al. (2019). Colonic epithelial cell diversity in health and inflammatory bowel disease. *Nature* **567**: 49–55. https://doi.org/10.1038/s41586-019-0992-y

Priem D, van Loo G, Bertrand M (2020). A20 and cell death-driven inflammation. *Trends in Immunology* **41**: 421–435. https://doi.org/10.1016/j.it.2020.03.001

Qi J, Kim J, Zhou Z, Lim C, Kim B (2020). Ferroptosis affects the progression of nonalcoholic steatohepatitis via the modulation of lipid peroxidation-mediated cell death in mice. *The American Journal of Pathology* **190**: 68–81. https://doi.org/10.1016/j.ajpath.2019.09.011

Rana N, Privitera G, Kondolf H, Bulek K, Lechuga S et al. (2022). GSDMB is increased in IBD and regulates epithelial restitution/repair independent of pyroptosis. *Cell* **185**: 283–298.e217. https://doi.org/10.1016/j.cell.2021.12.024

Seibt TM, Proneth B, Conrad M (2019). Role of GPX4 in ferroptosis and its pharmacological implication. *Free Radical Biology & Medicine* **133**: 144–152. https://doi.org/10.1016/j.freeradbiomed.2018.09.014

Singh S, Dulai PS, Zarrinpar A, Ramamoorthy S, Sandborn WJ (2017). Obesity in IBD: Epidemiology, pathogenesis, disease course and treatment outcomes. *Nature Reviews Gastroenterology & Hepatology* **14**: 110–121. https://doi.org/10.1038/nrgastro.2016.181

Stockwell BR, Friedmann Angeli JP, Bayir H, Bush AI, Conrad M et al. (2017). Ferroptosis: A regulated cell death nexus linking metabolism, redox biology, and disease. *Cell* **171**: 273–285. https://doi.org/10.1016/j.cell.2017.09.021

Stockwell BR, Jiang X (2020). The chemistry and biology of ferroptosis. *Cell Chemical Biology* **27**: 365–375. https://doi.org/10.1016/j.chembiol.2020.03.013

Subramanian S, Geng H, Tan XD (2020). Cell death of intestinal epithelial cells in intestinal diseases. *Sheng Li Xue Bao/Acta Physiologica Sinica* **72**: 308–324. https://doi.org/10.13294/j.aps.2020.0039

Xiao F, Zhang D, Wu Y, Jia Q, Zhang L, Li Y, Yang Y, Wang H, Wu C, Wang L (2019). miRNA-17-92 protects endothelial cells from erastin-induced ferroptosis through targeting the A20-ACSL4 axis. *Biochemical and Biophysical Research Communications* **515**: 448–454. https://doi.org/10.1016/j.bbrc.2019.05.147

Xie B, Guo Y (2021). Molecular mechanism of cell ferroptosis and research progress in regulation of ferroptosis by noncoding RNAs in tumor cells. *Cell Death Discovery* **7**: 101. https://doi.org/10.1038/s41420-021-00483-3

Xu S, He Y, Lin L, Chen P, Chen M, Zhang S (2021). The emerging role of ferroptosis in intestinal disease. *Cell Death & Disease* **12**: 289. https://doi.org/10.1038/s41419-021-03559-1

Yang WS, Stockwell BR (2016). Ferroptosis: Death by lipid peroxidation. *Trends in Cell Biology* **26**: 165–176. https://doi.org/10.1016/j.tcb.2015.10.014

Yin J, Wu M, Duan J, Liu G, Cui Z et al. (2015). Pyrrolidine dithiocarbamate inhibits NF-KappaB activation and upregulates the expression of Gpx1, Gpx4, Occludin, and ZO-1 in DSS-induced colitis. *Applied Biochemistry and Biotechnology* **177**: 1716–1728. https://doi.org/10.1007/s12010-015-1848-z

Zhang X, Wang Y, Ma Z, Liang Q, Tang X, Hu D, Tan H, Xiao C, Gao Y (2015). Tanshinone IIA ameliorates dextran sulfate sodium-induced inflammatory bowel disease via the pregnane X receptor. *Drug Design, Development and Therapy* **9**: 6343–6362. https://doi.org/10.2147/DDDT

Zhang X, Wang Q, Wang X, Chen X, Shao M et al. (2019). Tanshinone IIA protects against heart failure post-myocardial infarction via AMPKs/mTOR-dependent autophagy pathway. *Biomedicine & Pharmacotherapy* **112**: 108599. https://doi.org/10.1016/j.biopha.2019.108599

Zhu G, Wu X, Jiang S, Wang Y, Kong D, Zhao Y, Wang W (2022). The application of omics techniques to evaluate the effects of Tanshinone IIA on dextran sodium sulfate induced ulcerative colitis. *Molecular Omics* **18**: 666–676. https://doi.org/10.1039/D2MO00074A